Synthetic Aperture Imaging with a Virtual Source Element

C. H. Frazier and W. D. O'Brien, Jr.

Bioacoustics Research Laboratory, Department of Electrical and Computer Engineering, University of Illinois
405 N. Mathews Avenue, Urbana, IL 61801

Abstract— **Currently ultrasonic imaging is performed in one of two modes: conventional B-scan imaging with a focused transducer or array imaging using beamforming processing to achieve the focus. Conventional B-mode imaging suffers from a limited depth of focus while synthetic aperture imaging is limited by a low signal to noise ratio (SNR). A new technique has been proposed [1] that combines these two techniques to overcome the limited depth of focus. The new technique involves focusing the region beyond the focus of the transducer by considering the focus a virtual element. In this paper, the use of the focus as a virtual element is examined, considering the model for the focus as an element, the use of apodization weights to lower sidelobes, and the SNR of the processed image. Using data collected with tungsten wires in a waterbath, it was found that resolution comparable to the resolution at the focus could be achieved while obtaining an acceptable SNR. Apodization was found to lower the sidelobes, but only at the expense of lateral resolution. With these experiments, the virtual source has been shown to exhibit the same behavior as an actual transducer element in response to synthetic aperture processing techniques.**

I. INTRODUCTION

A basic limitation of conventional B-mode imaging is that lateral resolution depends on the depth in the image. The best resolution is achieved only for the slice of the image containing echoes from the focus of the transducer. In 1996, Passman and Ermert [1] introduced a technique to overcome this resolution limitation. The new technique involved treating the focus of the transducer as a virtual source for synthetic aperture (SA) processing. In their formulation, the virtual source was assumed to produce approximately spherical waves over a certain aperture angle.

This study examines the ability of known SA techniques to improve the quality of images created with a virtual source element. In particular, apodization weights are commonly applied to signals from individual elements before summing in order to reduce sidelobe levels in images. However, these weights also have the effect of increasing the main lobe width of the beam pattern, degrading the resolution of the image. This tradeoff between beamwidth and resolution is studied.

In addition, the electronic SNR of SA images is often unacceptable because individual elements do not output much power. SNR is studied to analyze whether or not it can be acceptable for images created with virtual sources.

II. BASIC PROCESSING

Synthetic aperture images created through delay and sum beamforming use the appropriate delay of returned signals to achieve focusing. The beamforming is accomplished with the sum in Equation (1) where the delays, Δt_i, are are calculated according to Equation (2)

$$A(t) = \sum_i w_i S_i(t - \Delta t_i) \tag{1}$$

$$\Delta t_i = \frac{2z}{c}\left(1 - \sqrt{1 + \frac{(id)^2}{z^2}}\right) \tag{2}$$

In Equation (1), $A(t)$ is the computed A-line, and w_i is a weight assigned to the returned signal, $S(t)$, from element i. The delay assigned to each element is determined geometrically. The goal is to make the received wave from the desired focal point arrive at each element simultaneously by delaying the signals with shorter round trip paths. In Equation (2), Δt_i is the time delay for element i, z is the distance to the desired focal point, c is the speed of sound, and d is the interelement spacing.

The aperture angle or angle of beam spread must be known before processing begins so that the number of received signals included in Equation 1 can be determined. A method for approximating the beam spread of the virtual source uses the focused beam shape. The initial beam spread after the focus is approximately equal to the degree of focusing before the spot. The aperture angle can then be approximated by the following expression

$$\sin(\frac{\phi}{2}) \approx \frac{D}{2F} \tag{3}$$

[1]This work was supported by NSF Fellowship and U.S. Army contract (DACA88-94-D0008).

where ϕ is the angle of the beam spread, D is the diameter of the transducer, and F is the distance to the transducer's focus. A comparison between the approximated and measured values for the transducers used in this study is presented below.

In SA imaging, it is desirable to have the transducer element as small as possible in order to obtain good resolution. When imaging with SA techniques, the received signals from several elements are added together. Only those elements whose beam patterns encompass the desired focal point should be included in the sum. If each element has a wide beam, then more of them will encompass the desired point. Therefore, the returned signals from more elements can be included in the sum, and the sampled aperture, which includes more elements, will be larger. Thus, the more highly focused the transducer, the better resolution will be achieved through synthetic aperture processing.

In this study, a C program is used to perform delay and sum beamforming with various apodization weights. After this processing, the data are transferred to Matlab for determination of the beamwidths, sidelobe levels, and SNR.

III. REDUCTION OF SIDELOBES

The tradeoff between resolution and peak sidelobe level is examined in this study. In array imaging, weighting the individual elements is known as apodization. In signal processing, the same process is called windowing. Signal processing theory shows that the windowing operation broadens the main lobe and lowers the sidelobes in a signal's frequency representation.

Several windows are used for this study. They are the boxcar window, the triangle, the cosine window, and the Hamming window. Characteristics of these windows are shown in Table 1. And the frequency representations of these windows are shown in Figure 1. From these descriptions, we expect the boxcar window to produce the image with the best resolution and the Hamming window to produce the image with the lowest sidelobes.

IV. DATA COLLECTION

Two Panametrics transducers with different focusing characteristics but focal points of similar size were used to collect the data for this study. The 15 MHz transducer has a 0.5 inch diameter circular aperture and a reported 0.75 inch focal distance giving it an f-number of 1.5. The 20 MHz transducer has a 0.25 inch diameter circular aperture and a 0.5 inch focal distance giving it an f-number of 2. The focal spot of each transducer is ideally 150 μm. According to the approximation for determining aperture angle, the 15 MHz transducer has an aperture angle of 39 degrees. Measurement of the beam spread shows that this transducer has an aperture angle of 42 degrees. Similarly, for the 20 MHz transducer the calculated aperture angle is 29 degrees while its measured aperture angle is 33 degrees.

Table 1: Window characteristics for length-M windows

Characteristics for Length-M Windows			
Window	Description	Main Lobe Width	Peak Sidelobe (dB)
boxcar	1	$\frac{4\pi}{M}$	-13
triangle	$1 - \left\|\frac{2(n-\frac{M-1}{2})}{M-1}\right\|$	$\frac{8\pi}{M}$	-27
cosine	$\cos(\frac{\pi}{2}\frac{n-\frac{M-1}{2}}{\frac{M-1}{2}})$	$\frac{20\pi}{3M}$	-23
Hamming	$0.54 - 0.46\cos\frac{2\pi n}{M-1}$	$\frac{8\pi}{M}$	-43

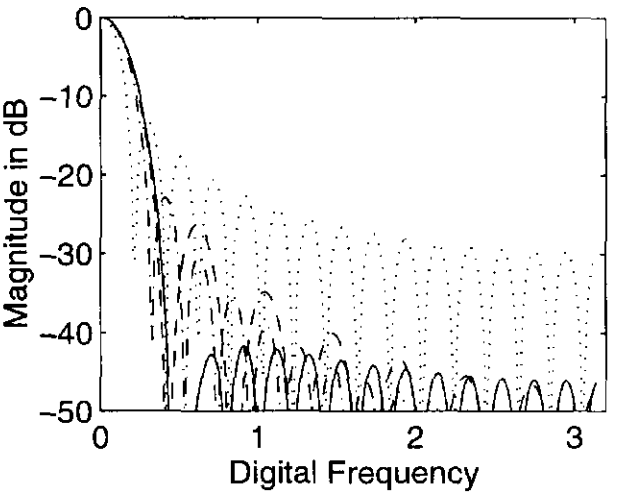

Figure 1: Frequency representation of apodization weights for the boxcar (dotted line), triangle (dashed line), cosine (dot-dashed line) and Hamming (solid line) windows.

Several B-scans of a 25 μm tungsten wire target in degassed water are created. Lateral scans are made using each transducer, with the wire target positioned at the focus and 3, 5, and 7 mm beyond the focus of the transducer. A-lines are collected 50 μm and 35 μm apart for the 15 MHz and 20 MHz transducers, respectively.

V. RESULTS

Typical wire images created by this technique are shown in Figure 2. The boxcar window produced the images with the best resolution for all the depths; however, the sidelobes were also the highest for all the depths compared to the other windows. The Hamming win-

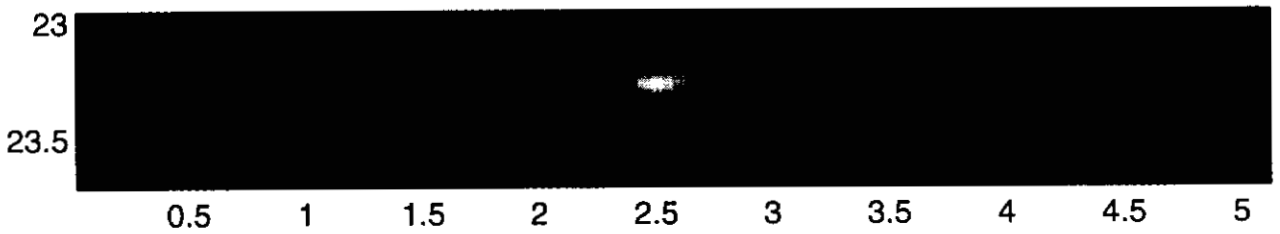

(a) Synthetic aperture processing using boxcar apodization weights

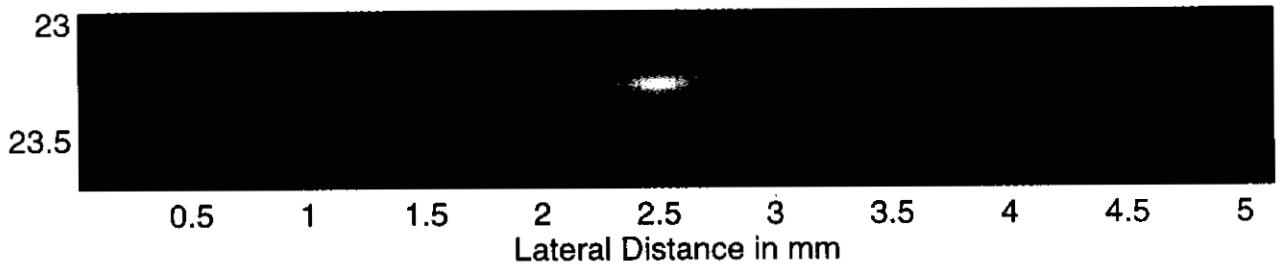

(b) Synthetic aperture processing using Hamming apodization weights

Figure 2: Images produced with synthetic aperture processing. The data are collected using the 15 MHz transducer with the wire positioned 5 mm beyond the focus.

dow produced the images with the lowest sidelobes and the worst lateral resolution. Images produced with the cosine window had slightly better resolution than those produced with the triangle window. Figure 3 plots the beamwidth of the main lobe versus depth with and without SA focusing using the boxcar window. The difference in the plots for no processing and with processing show the improvement in resolution that can be achieved by applying this technique. Ideally, with SA processing, the beamwidth should be independent of the depth. In Figure 4, the beamwidth of the mainlobe versus depth is plotted for data processed with the four apodization weights for the 20 MHz transducer. The results for the 15 MHz transducer are similar with slightly greater beamwidths. These beamwidths should be compared to the beamwidths at the focus of each transducer, which were found to be 157 and 159 μm for the 15 and 20 MHz transducers, respectively. The 15 MHz transducer has a larger aperture angle, so it can achieve a larger synthetic aperture, but the images produced with the 20 MHz transducer had better resolution due to the smaller wavelength.

The lateral resolution is degraded by the use of apodization weights; however, they are still used to lower the sidelobes in the beam pattern. Four beam patterns for the four different windows studied, are shown in Figure 5 for the wire at depth 3 mm from the focus using the 20 MHz transducer. The nonuniform weights lowered the

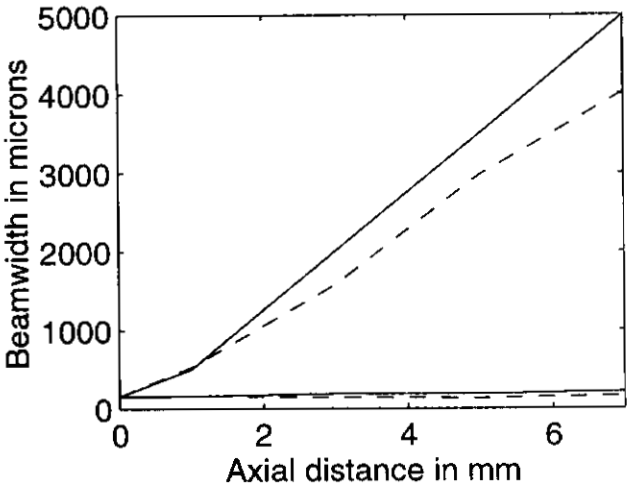

Figure 3: Comparison of beamwidth vs. depth before and after SA processing for the 15 MHz (solid lines) and 20 MHz (dashed lines) transducers.

sidelobes; however the improvement is more clear from the images shown in Figure 4 than from the plots of the beam patterns. Use of apodization weights reduced the wings that precede the wire in the image.

Finally SNRs were also calculated for the images. Assuming uncorrelated, additive electronic noise, the SNR of the processed image would ideally show an improve-

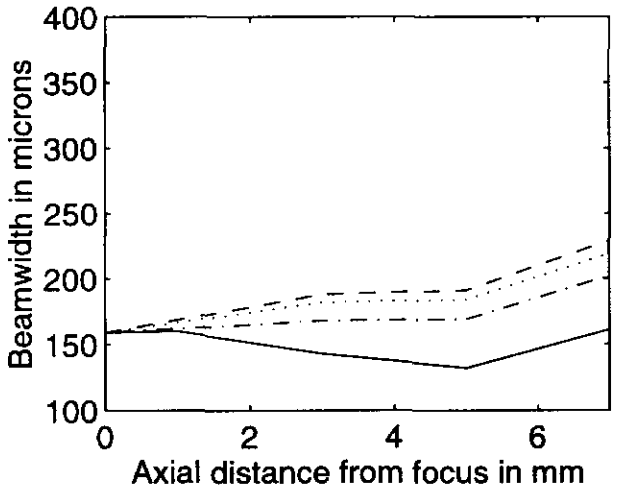

Figure 4: Comparison of beamwidth vs. depth after SA processing with boxcar (solid line), triangle (dotted line), cosine (dot-dashed line) and Hamming (dashed line) apodization weights for the 20 MHz transducer.

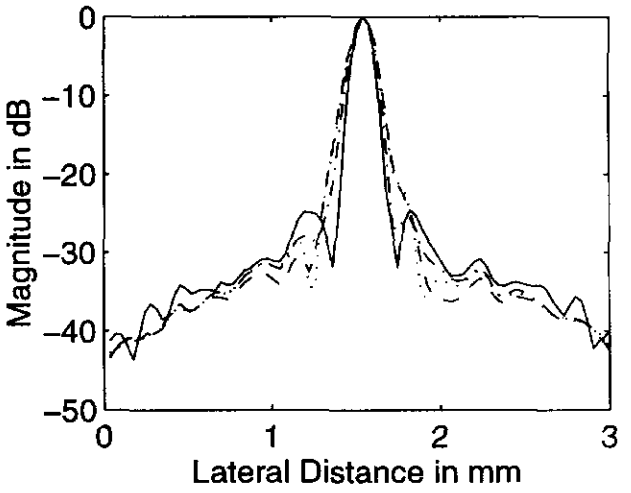

Figure 5: Beamplot at focus using boxcar (solid line), triangle (dotted line), cosine (dot-dashed line), and Hamming (dashed line) apodization weights.

ment over that of the original data of $10log_{10}(N)$ where N is the number of signals included in the sum to create a single A-line of the image. The results of these measurements and calculations are shown in Table 2. For comparison, the SNR computed for a conventional B-mode image with the wire at the focal depth of the 15 MHz transducer is 38.6 dB and for the 20 MHz transducer is 31.9 dB.

Table 2: SNR characteristics of the processed image

Measured and Calculated SNR				
Tdr (MHz)	Depth (mm)	Ideal Improvement (dB)	Single Element (dB)	Meas. SNR (dB)
15	3	13.22	24.85	33.53
	5	15.91	24.20	35.59
	7	17.56	28.03	39.39
20	3	16.13	26.55	30.08
	5	17.85	28.20	29.06
	7	19.40	27.50	35.20

The SNR showed less than the expected improvement, which results from errors in the delays or lower SNR in some received A-lines than the measured values. The values for the SNR of a single element presented in Table 2 are median values. Measured A-lines show a larger SNR when the wire is near the center of the beam than when the wire is at the edge of the beam. In any case, with a 40 dB receiver gain, the SNR is 34.1 dB on average, which is acceptable. The same experiment is repeated using 20 dB gain, which produced an unacceptable SNR of 19.7 dB on average. The two transducers show different improvement because more elements are included in the sum for the 20 MHz transducer. This transducer actually has a smaller beam spread, but the transducer positions were closer together because of the smaller wavelength.

VI. CONCLUSION

The behavior of a virtual source in response to synthetic aperture processing has been studied. The results show that it is possible to treat the focus of a transducer as a virtual element for the sake of SA processing. Once the beam pattern of the transducer has been determined, SA processing can be performed without regard to whether or not the element actually exists. To lower sidelobes, the modifications that have been made to delay and sum beamforming with actual elements can be applied to images created with virtual sources. The SNR can be close to the SNR for an image created with conventional B-mode imaging; however, the resolution is greatly improved for the SA images. The application of the result is not limited to medical imaging.

REFERENCES

[1] C. Passman and H. Ermert, "A 100 MHz ultrasound imaging system for dermatologic and ophthalmologic diagnostics," *IEEE Trans. Ultrason., Ferroelect., Freq. Cont.*, vol. 43, no. 4, pp.545-552, July 1996.